AJNR

Cortical Distribution of Fragile Periventricular Anastomotic Collateral Vessels in Moyamoya Disease: An Exploratory Cross-Sectional Study of Japanese Patients with Moyamoya Disease

A. Miyakoshi, T. Funaki, Y. Fushimi, T. Nakae, M. Okawa, T. Kikuchi, H. Kataoka, K. Yoshida, Y. Mineharu, M. Matsuhashi, E. Nakatani and S. Miyamoto

AJNR Am J Neuroradiol 2020, 41 (12) 2243-2249
doi: https://doi.org/10.3174/ajnr.A6861
http://www.ajnr.org/content/41/12/2243

Cortical Distribution of Fragile Periventricular Anastomotic Collateral Vessels in Moyamoya Disease: An Exploratory Cross-Sectional Study of Japanese Patients with Moyamoya Disease

A. Miyakoshi, T. Funaki, Y. Fushimi, T. Nakae, M. Okawa, T. Kikuchi, H. Kataoka, K. Yoshida, Y. Mineharu, M. Matsuhashi, E. Nakatani, and S. Miyamoto

ABSTRACT

BACKGROUND AND PURPOSE: Collateral vessels in Moyamoya disease represent potential sources of bleeding. To test whether these cortical distributions vary among subtypes, we investigated cortical terminations using both standardized MR imaging and MRA.

MATERIALS AND METHODS: Patients with Moyamoya disease who underwent MR imaging with MRA in our institution were enrolled in this study. MRA was spatially normalized to the Montreal Neurological Institute space; then, collateral vessels were measured on MRA and classified into 3 types of anastomosis according to the parent artery: lenticulostriate, thalamic, and choroidal. We also obtained the coordinates of collateral vessel outflow to the cortex. Differences in cortical terminations were compared among the 3 types of anastomosis.

RESULTS: We investigated 219 patients with Moyamoya disease, and a total of 190 collateral vessels (lenticulostriate anastomosis, $n = 72$; thalamic anastomosis, $n = 21$; choroidal anastomosis, $n = 97$) in 46 patients met the inclusion criteria. We classified the distribution patterns of collateral anastomosis as follows: lenticulostriate collaterals outflowing anteriorly ($P < .001$; 95% CI, 67.0–87.0) and medially ($P < .001$; 95% CI, 11.0–24.0) more frequently than choroidal collaterals; lenticulostriate collaterals outflowing anteriorly more frequently than thalamic collaterals ($P < .001$; 95% CI, 34.0–68.0); and choroidal collaterals outflowing posteriorly more frequently than thalamic collaterals ($P < .001$; 95% CI, 14.0–34.0). Lenticulostriate anastomoses outflowed to the superior or inferior frontal sulcus and interhemispheric fissure. Thalamic anastomoses outflowed to the insular cortex and cortex around the central sulcus. Choroidal anastomoses outflowed to the cortex posterior to the central sulcus and the insular cortex.

CONCLUSIONS: Cortical distribution patterns appear to differ markedly among the 3 types of collaterals.

ABBREVIATIONS: choA = choroidal artery; LSA = lenticulostriate artery; MNI = Montreal Neurological Institute; PcomA = posterior communicating artery

Collateral vessels in Moyamoya disease develop as the disease progresses.[1] Lenticulostriate arteries (LSAs), perforators from the posterior communicating artery (PcomA), and anterior and posterior choroidal arteries (choAs) are representative collateral vessels that supply the cortex.[2-4] Development of such collateral vessels represents a risk factor for intracerebral hemorrhage,[3,5-7] and these vessels have frequently been considered as the vessels responsible for bleeding in recent reports.[8-10] These collateral vessels connect with medullary arteries near the lateral ventricle and thus supply the cortex via the medullary arteries.[3,4] However, no reports have addressed the cortical distributions of these collateral vessels.

Bypass surgery reduces the risk of rebleeding in patients with hemorrhagic onset of Moyamoya disease[7,11-13] and also shrinks collateral vessels in Moyamoya disease.[7,12,14,15] Augmentation of cerebral blood flow via bypass seems to decrease the necessity for development of collateral flow and shrinks existing collaterals.[15] To shrink risky collateral vessels effectively and prevent hemorrhage, well-designed and planned bypass surgeries may be required.[16] Comprehension of the nature and cortical distribution of collateral vessels may thus be clinically useful.

Received May 1, 2020; accepted after revision August 6.

From the Departments of Neurosurgery (A.M., T.F., M.O., T.K., H.K., K.Y., Y.M., S.M.), Diagnostic Imaging and Nuclear Medicine (Y.F.), and Epilepsy, Movement Disorders and Physiology (M.M.), Kyoto University Graduate School of Medicine, Kyoto, Japan; Department of Neurosurgery (A.M.), and Division of Statistical Analysis (E.N.), Shizuoka General Hospital, Shizuoka, Japan; and Department of Neurosurgery (T.N.), Shiga General Hospital, Shiga, Japan.

Please address correspondence to Akinori Miyakoshi, MD, Department of Neurosurgery, Shizuoka General Hospital, Shizuoka, Japan, 4-27-1, Kita Ando, Aoi-ku Shizuoka City, Shizuoka, 420-8527, Japan; e-mail: myks-knr@umin.ac.jp

Indicates open access to non-subscribers at www.ajnr.org
Indicates article with supplemental on-line video.

http://dx.doi.org/10.3174/ajnr.A6861

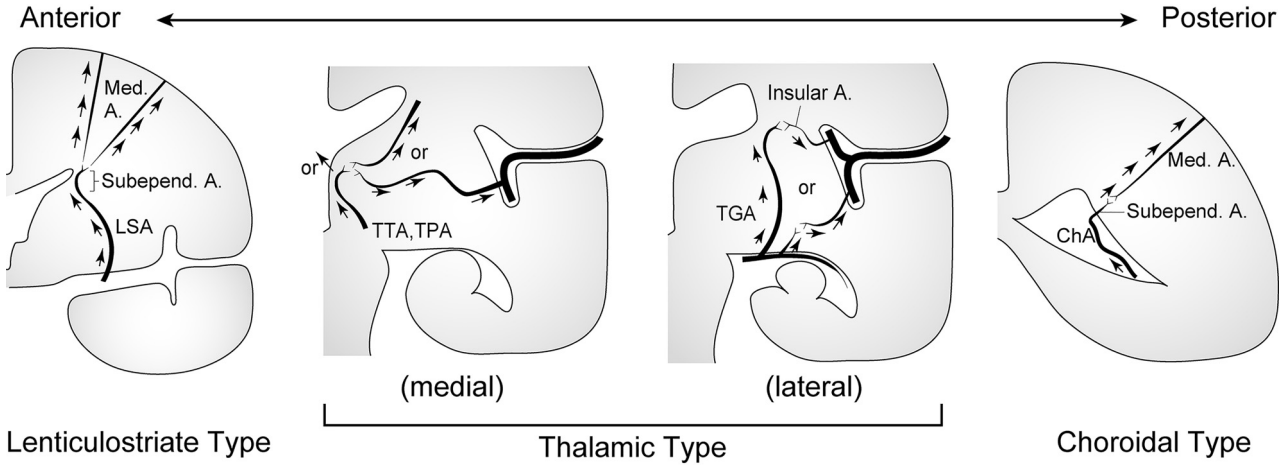

FIG 1. Schematic illustration showing a coronal plane of the left cerebral hemisphere and 3 subtypes of collateral anastomoses: lenticulostriate, thalamic, and choroidal anastomoses. A indicates artery; Med, medullary; Subepend, subependymal; TGA, thalamogeniculate artery; TPA, thalamoperforating artery; TTA, thalamotuberal artery. Reprinted with permission from Funaki et al.[18]

MRA performed using a 3T scanner has proved useful for detecting the abnormally extended collateral vessels in Moyamoya disease.[2] We investigated the cortical distribution of collateral vessels using 3T MR imaging and MRA to clarify whether cortical distributions vary among anastomotic subtypes and to better understand collateral networks.

MATERIALS AND METHODS

Study Design and Patients

This investigation was designed as a cross-sectional study. The study protocols were reviewed and approved by the ethics committee at the Kyoto University Graduate School of Medicine (R1600). Informed consent was obtained by an opt-out method on the institutional Web site. In accordance with the ethical standards of the institutional and national research committees, this retrospective, noninvasive study did not require formal consent. Instead, the outline of the study was open to the public on the institutional homepage and provided an opportunity for patients to decline to participate in the research. We retrospectively enrolled consecutive patients diagnosed with Moyamoya disease who visited our institution between January 2009 and April 2018. The diagnosis of Moyamoya disease was determined according to the proposed criteria.[1] Patients were excluded from the analysis if they had been diagnosed with quasi-Moyamoya disease (secondary Moyamoya phenomenon due to underlying disease). Patients who had undergone craniotomy (ie, hematoma-evacuation craniotomy or indirect or direct bypass surgery) were excluded, as were cases in which brains showed a change in shape from a normal structure because of massive infarction or hemorrhage. This exclusion was because an abnormal structure of the brain was considered to affect standardization of the brain. Patients who had not undergone imaging that met the imaging protocols were also excluded.

Imaging Protocol and Postimaging Processing

A 3T MR imaging scanner (Magnetom Trio, Skyra, or Prisma; Siemens) using a 32-channel head coil was introduced in 2009. Whole-brain 3D-T1WI was performed in all cases for anatomic standardization. Imaging parameters for 3D-T1WI and TOF-MRA in this study were as follows—T1-weighted MPRAGE: TR, 1900 ms; TE, 2.58 ms; flip angle, 9°; TI, 900 ms; FOV, 230 × 230 mm; matrix, 256 × 256; section thickness, 0.9 mm; generalized auto calibrating partially parallel acquisitions, 2; scan time, 4 minutes 26 seconds; TOF-MRA: TR, 20–21 ms; TE, 3.69 ms; flip angle, 20°; FOV, 220 × 187 mm; matrix, 384 × 328; section thickness, 0.7 mm; generalized auto calibrating partially parallel acquisitions, 3; scan time, 5 minutes 48 seconds. The imaging field extended from the level of the foramen magnum to the top of the head.

Images from MRA were registered to the corresponding T1WI. Subsequently, images from 3D-T1WI and MRA were anatomically standardized into the Montreal Neurological Institute (MNI) space using SPM12 software (https://www.fil.ion.ucl.ac.uk/spm/). To retain vessel information from MRA, we applied a 0.5-mm Gaussian smoothing kernel to these spatially normalized images from T1WI and MRA. Thus, all images from T1WI and MRA were created as 0.5-mm isotropic images in MNI coordinates.

Measurement of Collateral Vessels That Are Continuously Detectable from Origin to the Cortex

We placed standardized MRA and T1WI from all axial, coronal, and sagittal views obtained in the same scanning session on the viewer of ITK-SNAP, Version 3.6, software (https://www.itksnap.org/).[17] Next, we detected collateral anastomoses on MRA and included collateral vessels for which signals could be identified all the way from the origin to the cerebral cortex without interruption. We classified the origin of anastomosis in 3 types (LSA, PcomA, or choA) on MRA according to previous reports[2,18] (Fig 1) and identified the point at which the anastomosis outflowed to the cortex. In brief, these types were the following: 1) lenticulostriate anastomosis, beginning at an LSA and connecting to the medullary or insular arteries; 2) thalamic anastomosis, beginning at the thalamotuberal, thalamoperforating, or thalamogeniculate arteries and connecting to the medullary or insular arteries; and 3) choroidal anastomosis, beginning at the anterior or posterior choroidal arteries and connecting to medullary or insular arteries. Thin-section T1WI was more favorable for detecting the edge of the cortex than MRA. Voxel coordinates of the outflow point were recorded, and the type

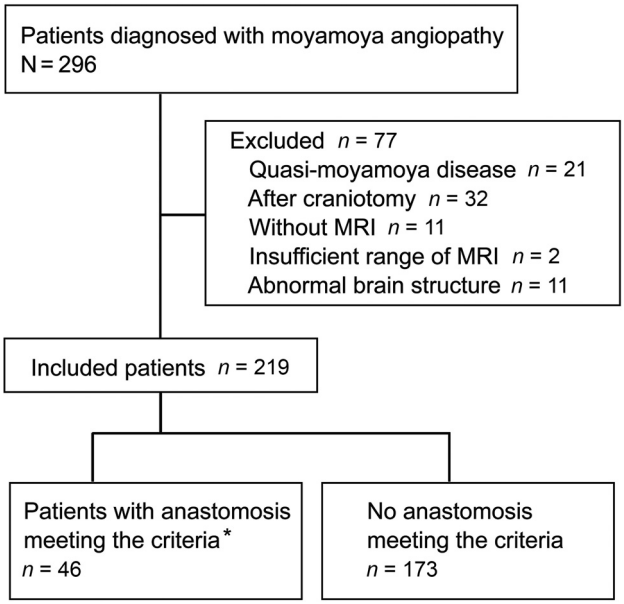

FIG 2. Flowchart for patient inclusion. *Asterisk* indicates that the patients have the anastomoses for which signals could be identified all the way from the origin to the cerebral cortex without interruption on MR angiography.

Patient characteristics

	Included Patients with Moyamoya Disease (*n* = 46)
Median age (range) (yr)	28.5 (3–56)
Male sex (No.) (%)	14 (30.4)
Clinical presentation (No.) (%)	
Ischemic symptoms	28 (60.9)
Hemorrhagic symptoms	11 (23.9)
Other symptoms	7 (15.2)

of anastomosis was classified according to the consensus decision of 2 neurosurgeons (A.M. and T.F.). An independent neuroradiologist (Y.F.) then identified the anastomosis on the basis of the coordinates recorded by the 2 neurosurgeons, tracked its signal to the origin, and then classified the type of anastomosis. In cases of disagreement between the neurosurgeons and the neuroradiologist, another neurosurgeon (M.O.) judged the type of anastomosis. In cases of an anastomosis joined to another type of anastomosis, we counted the case as 2 anastomoses for 1 outflow point. Interrater agreement for the origin of collateral vessels between the consensus decision of the 2 neurosurgeons and the neuroradiologist was then evaluated. The actual measurement process is shown in the Online Video.

Voxel coordinates on ITK-SNAP ranged from 1 to 361 (right to left) for the x-axis, 1 to 395 (back to front) for the y-axis, and 1 to 345 (caudal to cranial) for the z-axis. To treat all coordinates as being on the left hemisphere, we performed a horizontal mirroring of coordinates—that is, we calculated x-axis coordinates on the right hemisphere as 362 – x.

Mapping Cortical Distribution of Perforating Arteries onto the Standardized Brain Model

Once we determined the cortical distributions of collateral arteries in individual brains, we converted voxel coordinates into the MNI space. For visualization in 3D space, we created a standard brain surface model from the T1WI provided as MNI152_T1_2mm_brain.nii.gz in the FSL package (https://fsl.fmrib.ox.ac.uk/fsl/fslwiki/FSL). To obtain an isosurface of the standard brain, we chose a threshold of 5400 to visualize sulci keeping the visibility of the cerebral cortex. The surface model was loaded and displayed in 3D, together with the coordinates of cortical distributions. These procedures were performed by our in-house script in Matlab software (MathWorks).

Statistical Analysis

Interrater agreement for the classification of collateral vessels between the consensus decision of the neurosurgeons (A.M. and T.F.) and the decision of the neuroradiologist (Y.F.) was evaluated using the unweighted κ statistic and the corresponding 95% CI. We compared x, y, and z voxel coordinates among the 3 types of anastomoses to evaluate differences in distributions. The Kruskal-Wallis test was used to compare the 3 types of anastomoses, and the Mann-Whitney *U* test was used for every 2 anastomoses using Bonferroni-corrected *P* values. $P < .05$ was considered significant in κ statistics and the Kruskal-Wallis test, and $P < .016$ (ie, .05/3) was used for the Mann-Whitney *U* test. We assumed that measurements from each anastomosis were independent along with patient characteristics and performed statistical analyses. All statistical analyses were conducted using R statistical and computing software, Version 3.5.2 (http://www.r-project.org).

RESULTS

Patients and Anastomoses

Between January 2009 and April 2018, a total of 296 patients diagnosed with Moyamoya disease visited our institution. Seventy-seven patients were excluded (quasi-Moyamoya disease, $n = 21$; after craniotomy including bypass surgery, $n = 32$; patients who had not undergone MR imaging, $n = 11$; insufficient range of MR imaging, $n = 2$; and abnormal brain structure, $n = 11$). We investigated the remaining 219 patients, with 46 of these 219 patients showing anastomoses for which uninterrupted signals could be identified all the way from the origin to the cerebral cortex (Fig 2).

A total of 190 anastomoses (lenticulostriate anastomosis, $n = 72$; thalamic anastomosis, $n = 21$; choroidal anastomosis, $n = 97$) were detected in 46 Japanese patients. Six anastomoses were counted as 2 different types of anastomosis joined (lenticulostriate and thalamic, $n = 2$; lenticulostriate and choroidal, $n = 2$; thalamic and choroidal, $n = 2$). Interrater agreement for the judgment of anastomosis origin was high ($\kappa = 0.95$; 95% CI, 0.90–0.99). Six cases showed a discrepancy in the judgment between the neurosurgeons and the neuroradiologist. As examples, 4 anastomoses counted as a lenticulostriate type by neurosurgeons had been classified as a choroidal type by the neuroradiologist. Those 4 anastomoses were finally judged as lenticulostriate types by the final neurosurgeon.

Background Characteristics of Patients

Fourteen male and 32 female patients with Moyamoya disease were included (median age, 28.5 years; range, 3–56 years) (Table). Among 46 patients, 28 patients had ischemic symptoms at onset, 11

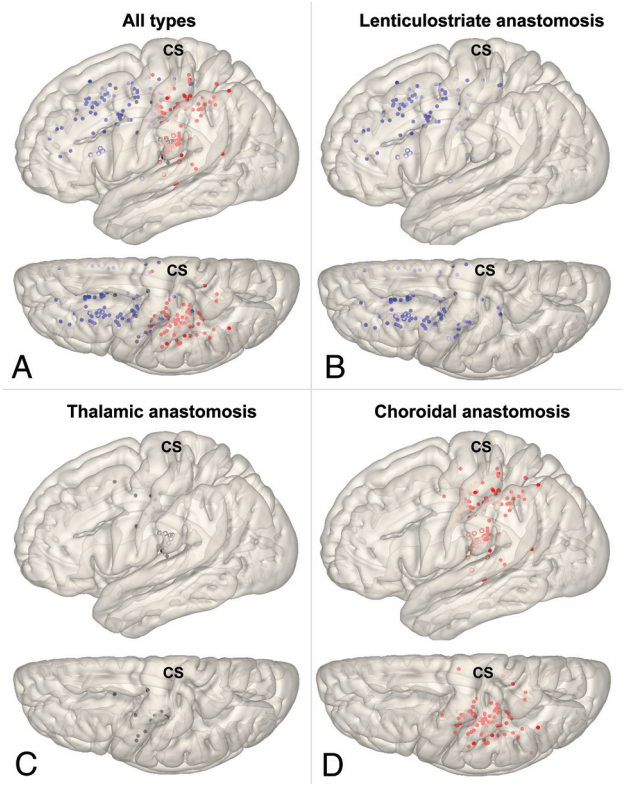

FIG 3. Cortical distributions for each type of collateral depicted on a standard brain surface model (*A*, All types; *B*, Lenticulostriate anastomosis; *C*, Thalamic anastomosis; *D*, Choroidal anastomosis). Each dot shows the point of anastomosis outflow to the cortex (*blue dot*, lenticulostriate anastomosis; *black dot*, thalamic anastomosis; *red dot*, choroidal anastomosis). *Unfilled circles* represent outflow on the insular cortex. *Pale dots* represent outflow located in a sulcus. CS indicates central sulcus.

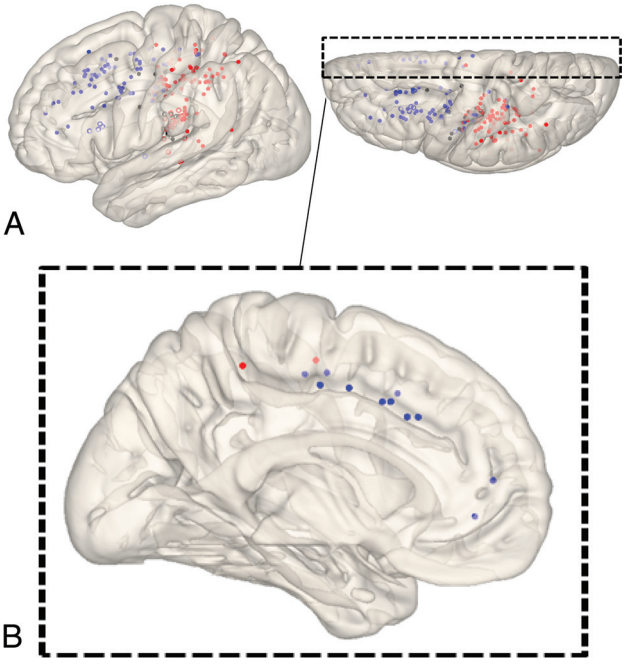

FIG 4. Cortical distributions of each type of collateral depicted on a standard brain surface model. Each *dot* shows the point where each anastomosis outflowed to the cortex (*blue dot*, lenticulostriate anastomosis; *black dot*, thalamic anastomosis; *red dot*, choroidal anastomosis). *White circles* (*circles without fill*) show *dots* located on the insular cortex. *A*, All *dots* are depicted on a brain surface model. *B*, The view from the medial surface of a 3D brain surface model. *Dots* were extracted that exist within 15 mm from the midline.

from hemorrhagic symptoms, with the remaining 7 patients presenting with other symptoms.

Cortical Distributions of Collateral Types on the Brain Surface

We demonstrated spatial distribution patterns of the "collateral anastomosis" or collateral vessels reaching the cerebral cortex without interruption. Cortical distributions of each type of collateral on the standard brain surface model are depicted in Figs 3 and 4. Lenticulostriate anastomoses developed from LSAs and showed outflow mainly to the superior and inferior frontal sulcus and cingulate sulcus (interhemispheric fissure) via medullary arteries. Thalamic anastomoses developed from PcomA perforators and showed outflow to the insular cortex and sulcus around the central sulcus via medullary arteries. Choroidal anastomoses developed from the anterior and posterior choroidal arteries and showed outflow to the sulci posterior to the central sulcus and the insular cortex via the medullary arteries.

Spatial Distribution Patterns of Collateral Anastomoses

For the x-axis (mediolateral direction), distributions among the 3 types of anastomosis differed significantly ($P < .001$). LSA anastomoses showed outflow to the cortex more medially than choroidal anastomoses ($P < .001$; 95% CI, 11.0–24.0) (Fig 5). For the y-axis (posterior-anterior direction), distributions among the 3 types of anastomosis also differed significantly ($P < .001$). LSA anastomoses showed outflow to the cortex more anteriorly than thalamic ($P < .001$; 95% CI, 34.0–68.0) or choroidal anastomoses ($P < .001$; 95% CI, 67.0–87.0) (Fig 6). Thalamic anastomoses showed outflow to the cortex more anteriorly than choroidal anastomoses ($P < .001$; 95% CI, 14.0–34.0) (Fig 6). For the z-axis (caudocranial direction), no significant differences in distribution were evident among the 3 types (Fig 7).

DISCUSSION

We demonstrated that lenticulostriate anastomoses showed outflow to the cortex more anteriorly and medially than choroidal anastomoses. Choroidal anastomoses showed outflow to the cortex more posteriorly than thalamic or lenticulostriate anastomoses.

We finally analyzed data from 46 of 219 patients with Moyamoya disease. The detection rate of abnormally dilated collaterals using MRA is equal to that using conventional DSA, as previously reported.[10] MRA is also superior for identifying positions of vessels relative to the brain. However, we processed MRA data to standardize the images using software, and this process slightly decreased the spatial resolution. We, therefore, only included obviously dilated collaterals with uninterrupted signals. This was 1 reason why most of the initial patient cohort was excluded.

Unlike the PcomA and choAs, abnormal dilation and extension of the LSA has not been proved to be associated with intracranial hemorrhage in Moyamoya disease. Two previous studies

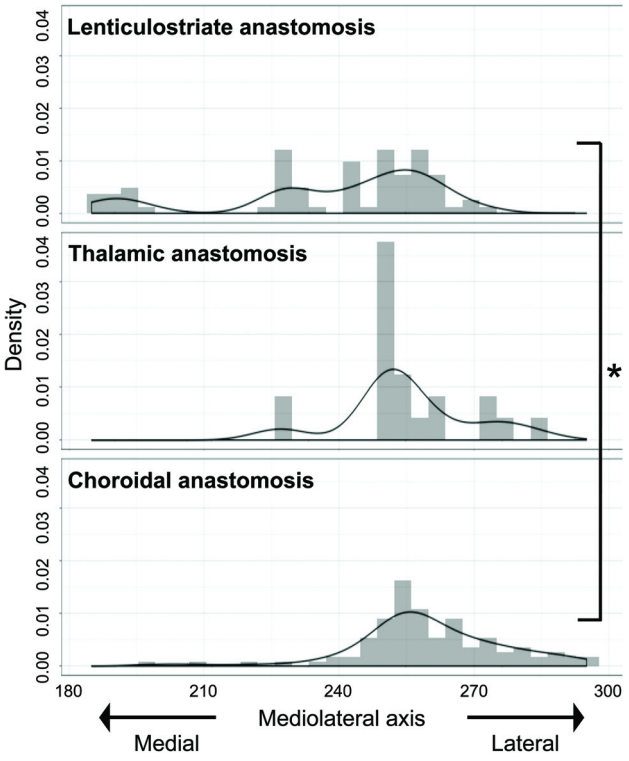

FIG 5. Mediolateral (x-coordinate) distribution of outflow to the cortex for each type of anastomosis. The value for the midline of images is 181, and the value for the lateral edge of images is 361. Values for x-coordinates are shown as density estimations. The *asterisk* indicates $P < .001$.

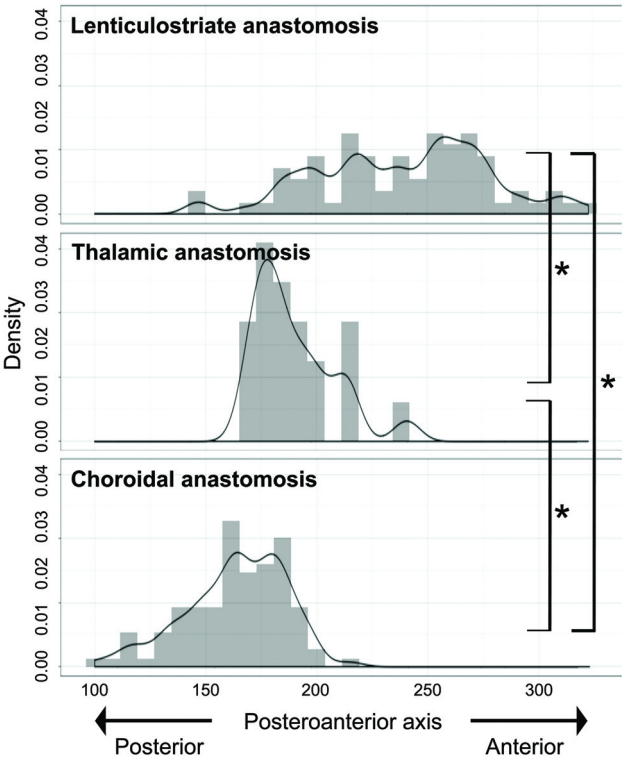

FIG 6. Posteroanterior (y-coordinate) distribution of outflow to the cortex for each type of anastomosis. The value for the posterior edge of images is 1, and the value for the frontal edge of images is 395. Values for y-coordinates are shown as density estimations. The *asterisk* indicates $P < .001$.

compared the development of LSA collaterals between ischemic- and hemorrhagic-onset Moyamoya disease, and no significant difference in the development of LSA collaterals was identified, unlike PcomA and choA collaterals.[4,19] However, a dilated and extended LSA is suggested as a vessel responsible for hemorrhage.[10] Some reports have also discussed ruptured aneurysms arising on dilated and extended LSAs.[9,20,21] These aneurysms supposedly develop due to an increase in the hemodynamic burden, to supply the cortex via collaterals in place of shrunken major arteries.[9,20,21] Furthermore, Takahashi et al[22] estimated LSAs as possible sources of anterior hemorrhage in a subanalysis of the Japan Adult Moyamoya Trial. Such findings suggest that lenticulostriate anastomosis is associated with anterior hemorrhage in Moyamoya disease.[3,22] Prospective cohort studies are expected to clarify the potential risk of LSA dilation in patients with Moyamoya disease.

Thalamic anastomosis was the least-detected anastomosis (21/190) among the 3 types of anastomosis seen in this study. Dilation and extension of the PcomA and its perforators represent a risk factor for hemorrhage in patients with Moyamoya disease.[5,7,19] Furthermore, a recent study suggested that dilated thalamic perforators represented a source of thalamic hemorrhage.[10] In the present study, thalamic anastomoses mainly showed outflow to the insular cortex, and less commonly to the cortex without joining with other types of anastomosis. Matsushige et al[23] evaluated the collateral networks in 15 patients with Moyamoya disease using 7T MRA and classified anastomoses of the thalamic perforators as PcomA perforators anastomosing with thalamostriate arteries and intrathalamic anastomoses among thalamic arteries. Those findings suggest that thalamic perforators less commonly outflow to the cortex independently and tend to anastomose with other collateral vessels. Thalamic collaterals might be strongly involved in thalamic hemorrhage[10] and may be less involved in periventricular hemorrhage at sites other than the thalamus.

In hemorrhagic-onset Moyamoya disease, choroidal anastomosis is the most frequently detected type of anastomosis and represents a strong risk factor for rebleeding.[3,6,7,24] Recent studies have suggested choroidal anastomosis as a risk factor for de novo hemorrhage in Moyamoya disease,[8] and choroidal anastomosis is mainly associated with posterior hemorrhage and periventricular hemorrhage in Moyamoya disease.[8,10,25] On the other hand, choroidal anastomoses frequently shrink after bypass surgery,[7,14,15] though the reasons remain poorly understood. We hypothesize that choroidal anastomoses may outflow to the cortex around the recipient site for ordinary bypass surgery. Collateral flow via direct bypass is thought to reduce the burden on abnormally developed collateral vessels and thus contribute to prevention of rebleeding.[3,7,13,15] On the basis of this concept, the anastomotic site of bypass might affect such preventative effects. In this study, choroidal anastomoses showed outflow to the cortex posterior to the central sulcus, in an area corresponding to the recipient site in bypass surgery.[26-29]

Takahashi et al[22] reported that the preventative effects of bypass surgery on rebleeding were not detected in an anterior hemorrhage group. The area of lenticulostriate anastomosis

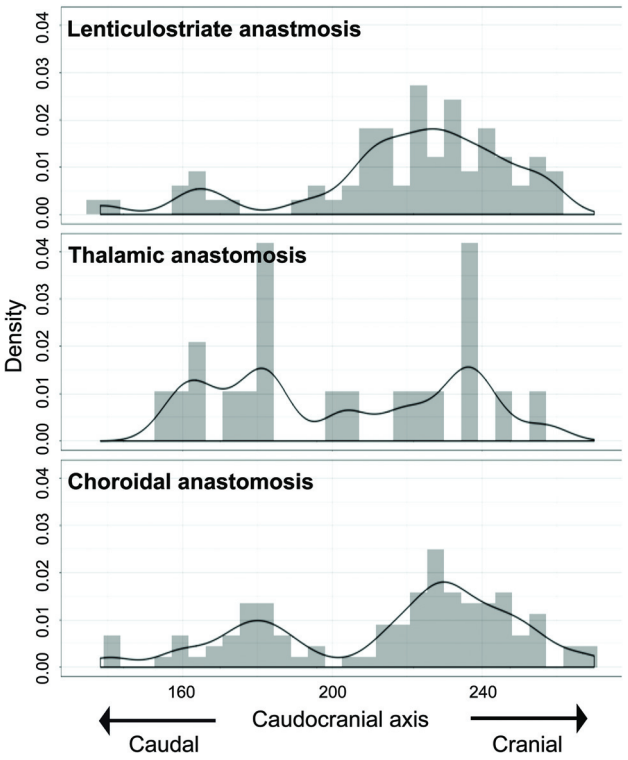

FIG 7. Caudocranial (z-coordinate) distribution of outflow to the cortex for each type of anastomosis. The value for the caudal edge of images is 1, and the value for the cranial edge of images is 345. Values for z-coordinates are shown as density estimations.

outflow is less likely to be the recipient site under usual bypass surgery because outflow is more anterior or to the interhemispheric fissure, unlike other anastomoses. This anatomic feature may explain the lack of preventative effects from bypass surgery among the anterior hemorrhage group.

Some limitations to this study must be considered. First, although we used spatially standardized MR imaging, anatomic differences in each patient would likely have had a small effect on the results. Second, although interrater agreement was high, both misclassification (measurement error) and observer bias are essential limitations and may have impacted the internal validity of this study. Third, although we analyzed 190 anastomoses in 46 patients among the cohort of 219 patients, these patients might represent an insufficient cohort to allow generalization of the results. Fourth, because all patients in this study were of Japanese ethnicity, the results are most generalizable to Japanese or Asian patients. Differences in the development of collateral vessels between Japanese and European white patients have already been reported.[30]

We believe the findings obtained from this study will contribute to understanding the pathology of hemorrhagic Moyamoya disease and to the establishment of better bypass surgeries to prevent bleeding among patients with Moyamoya disease.

CONCLUSIONS

Outflow of lenticulostriate anastomoses was more anterior than that of thalamic and choroidal anastomoses. Outflow of lenticulostriate anastomoses was more medial than that of choroidal anastomoses. Outflow of choroidal anastomoses was more posterior than that of lenticulostriate and thalamic anastomoses. Lenticulostriate anastomosis outflow to the cortex was anterior to the central sulcus and to the interhemispheric fissure. Thalamic anastomosis outflow was to the insular cortex and cortex around the central sulcus. Choroidal anastomosis outflow was to the cortex posterior to the central sulcus and the insular cortex. A more detailed understanding of each pattern of cortical distribution from abnormal collateral vessels may contribute to designing treatment strategies, allowing tailored bypass surgery optimized to prevent hemorrhage among patients with Moyamoya disease.[16]

Disclosures: Masao Matsuhashi—*RELATED: Grant*: KAKENHI, *Comments*: Ministry of Education, Culture, Sports, Science and Technology KAKENHI grant No. 15H05875; *UNRELATED*: *Grants/Grants Pending*: KAKENHI, *Comments*: 19H03574, 19H01091, 18H02709, 17H02121, 26330175, 21700288; *OTHER RELATIONSHIPS*: Department of Epilepsy, Movement Disorders and Physiology, Kyoto University, is the Industry-Academia Collaboration Courses, supported by Eisai Co, Nihon Kohden Corp, Otsuka Pharmaceutical Co, and UCB Japan Co. Eiji Nakatani—*UNRELATED*: *Consultancy*: Sagamihara National Hospital, Osaka University; *Expert Testimony*: Osaka University; *Grants/Grants Pending*: Shionogi & Co. Shizuoka Prefecture, Japan Society for the Promotion of Science*; *Payment for Lectures Including Service on Speakers Bureaus*: Celgene Japan. *Money paid to the institution.

REFERENCES

1. Research Committee on the Pathology and Treatment of Spontaneous Occlusion of the Circle of Willis; Health Labour Sciences Research Grant for Research on Measures for Infractable Diseases. **Guidelines for diagnosis and treatment of moyamoya disease (spontaneous occlusion of the circle of Willis).** *Neurol Med Chir (Tokyo)* 2012;52:245–66 CrossRef Medline
2. Funaki T, Takahashi JC, Yoshida K, et al. **Periventricular anastomosis in moyamoya disease: detecting fragile collateral vessels with MR angiography.** *Japan Neurosurg* 2016;124:1766–72 CrossRef Medline
3. Funaki T, Takahashi JC, Houkin K, et al. **Angiographic features of hemorrhagic moyamoya disease with high recurrence risk: a supplementary analysis of the Japan Adult Moyamoya Trial.** *J Neurosurg* 2018;128:777–84 CrossRef Medline
4. Yamamoto S, Hori S, Kashiwazaki D, et al. **Longitudinal anterior-to-posterior shift of collateral channels in patients with moyamoya disease: an implication for its hemorrhagic onset.** *J Neurosurg* 2018;130:884–90 CrossRef Medline
5. Morioka M, Hamada JI, Kawano T, et al. **Angiographic dilatation and branch extension of the anterior choroidal and posterior communicating arteries are predictors of hemorrhage in adult moyamoya patients.** *Stroke* 2003;34:90–95 CrossRef Medline
6. Liu P, Han C, Li DS, et al. **Hemorrhagic moyamoya disease in children: clinical, angiographic features, and long-term surgical outcome.** *Stroke* 2016;47:240–43 CrossRef Medline
7. Jiang H, Ni W, Xu B, et al. **Outcome in adult patients with hemorrhagic moyamoya disease after combined extracranial-intracranial bypass.** *J Neurosurg* 2014;121:1048–55 CrossRef Medline
8. Funaki T, Takahashi JC, Houkin K, et al. **Effect of choroidal collateral vessels on de novo hemorrhage in moyamoya disease: analysis of nonhemorrhagic hemispheres in the Japan Adult Moyamoya Trial.** *J Neurosurg* 2019;132:408–14 CrossRef Medline
9. Sasagasako T, Funaki T, Tanji M, et al. **Intractable medial anastomotic branches from the lenticulostriate artery causing recurrent hemorrhages in moyamoya disease.** *World Neurosurg* 2019;127:279–83 CrossRef Medline
10. Miyakoshi A, Funaki T, Fushimi Y, et al. **Identification of the bleeding point in hemorrhagic moyamoya disease using fusion images of susceptibility-weighted imaging and time-of-flight MRA.** *AJNR Am J Neuroradiol* 2019;40:1674–80 CrossRef Medline

11. Miyamoto S, Yoshimoto T, Hashimoto N; et al; JAM Trial Investigators. **Effects of extracranial-intracranial bypass for patients with hemorrhagic moyamoya disease: results of the Japan Adult Moyamoya Trial.** *Stroke* 2014;45:1415–21 CrossRef Medline
12. Liu X, Zhang D, Shuo W, et al. **Long-term outcome after conservative and surgical treatment of haemorrhagic moyamoya disease.** *J Neurol Neurosurg Psychiatry* 2013;84:258–65 CrossRef Medline
13. Jang DK, Lee KS, Rha HK, et al. **Bypass surgery versus medical treatment for symptomatic moyamoya disease in adults.** *J Neurosurg* 2017;127:492–502 CrossRef Medline
14. Irikura K, Miyasaka Y, Kurata A, et al. **The effect of encephalo-myosynangiosis on abnormal collateral vessels in childhood moyamoya disease.** *Neurol Res* 2000;22:341–46 CrossRef Medline
15. Miyakoshi A, Funaki T, Takahashi JC, et al. **Restoration of periventricular vasculature after direct bypass for moyamoya disease: intra-individual comparison.** *Acta Neurochir* 019;161:947–54 CrossRef Medline
16. Funaki T, Kataoka H, Yoshida K, et al. **The targeted bypass strategy for preventing hemorrhage in moyamoya disease: technical note.** *Neurol Med Chir (Tokyo)* 2019;59:517–22 CrossRef Medline
17. Yushkevich PA, Piven J, Hazlett HC, et al. **User-guided 3D active contour segmentation of anatomical structures: significantly improved efficiency and reliability.** *Neuroimage* 2006;31:1116–28 CrossRef Medline
18. Funaki T, Fushimi Y, Takahashi JC, et al. **Visualization of periventricular collaterals in moyamoya disease with flow-sensitive black-blood magnetic resonance angiography: preliminary experience.** *Neurol Med Chir (Tokyo)* 2015;55:204–09 CrossRef Medline
19. Fujimura M, Funaki T, Houkin K, et al. **Intrinsic development of choroidal and thalamic collaterals in hemorrhagic-onset moyamoya disease: case-control study of the Japan Adult Moyamoya Trial.** *J Neurosurg* 2019;130:1453–59 CrossRef Medline
20. Liu P, Lv XL, Liu AH, et al. **Intracranial aneurysms associated with moyamoya disease in children: clinical features and long-term surgical outcome.** *World Neurosurg* 2016;94:513–20 CrossRef Medline
21. Ni W, Jiang H, Xu B, et al. **Treatment of aneurysms in patients with moyamoya disease: a 10-year single-center experience.** *J Neurosurg* 2018;128:1813–22 CrossRef Medline
22. Takahashi JC, Funaki T, Houkin K, et al; JAM Trial Investigators. **Significance of the hemorrhagic site for recurrent bleeding: prespecified analysis in the Japan Adult Moyamoya Trial.** *Stroke* 2016;47:37–43 CrossRef Medline
23. Matsushige T, Kraemer M, Sato T, et al. **Visualization and classification of deeply seated collateral networks in moyamoya angiopathy with 7T MRI.** *AJNR Am J Neuroradiol* 2018;39:1248–54 CrossRef Medline
24. Funaki T, Takahashi JC, Houkin K, et al. **High rebleeding risk associated with choroidal collateral vessels in hemorrhagic moyamoya disease: analysis of a nonsurgical cohort in the Japan Adult Moyamoya Trial.** *J Neurosurg* 2019;130:525–30 CrossRef Medline
25. Wang J, Yang Y, Li X, et al. **Lateral posterior choroidal collateral anastomosis predicts recurrent ipsilateral hemorrhage in adult patients with Moyamoya disease.** *AJNR Am J Neuroradiol* 2019;40:1665–71 CrossRef Medline
26. Guzman R, Steinberg GK. **Direct bypass techniques for the treatment of pediatric moyamoya disease.** *Neurosurg Clin N Am* 2010;21:565–73 CrossRef Medline
27. Houkin K, Kamiyama H, Takahashi A, et al. **Combined revascularization surgery for childhood moyamoya disease: STA-MCA and encephalo-duro-arterio-myo-synangiosis.** *Childs Nerv Syst* 1997;13:24–29 CrossRef Medline
28. Kim DS, Yoo DS, Huh PW, et al. **Combined direct anastomosis and encephaloduroarteriogaleosynangiosis using inverted superficial temporal artery-galeal flap and superficial temporal artery-galeal pedicle in adult moyamoya disease.** *Surg Neurol* 2006;66:389–94 CrossRef Medline
29. Acker G, Fekonja L, Vajkoczy P. **Surgical management of Moyamoya disease.** *Stroke* 2018;49:476–82 CrossRef Medline
30. Hori S, Kashiwazaki D, Yamamoto S, et al. **Impact of interethnic difference of collateral angioarchitectures on prevalence of hemorrhagic stroke in Moyamoya disease.** *Neurosurgery* 2019;85:134–46 CrossRef Medline